

“Remote” Fabrication via Three-Dimensional Reaction-Diffusion: Making Complex Core-and-Shell Particles and Assembling Them into Open-Lattice Crystals

By Paul J. Wesson, Siowling Soh, Rafal Klajn, Kyle J. M. Bishop, Timothy P. Gray, and Bartosz A. Grzybowski*

Despite enormous progress in microfabrication techniques,^[1–3] preparation of mesoscopic (micrometers to millimeters) core-and-shell particles (CSP) remains technically challenging. Surface tension effects can be used to fabricate various types of spherical or spheroidal CSPs (e.g., using microfluidic encapsulation^[4–8] or folding of prepolymer patches in the effective absence of gravity^[9]), but cannot be easily extended to particles, in which the symmetries of the entire particle and of its internal component(s) are different. For example, it is currently relatively easy to make a spherical particle containing one or more smaller spheres,^[4,5] but it is rather hard to make a polyhedron containing a sphere. In this paper, we describe a method of fabricating such symmetry “mismatched” CSPs by reaction-diffusion (RD) in either aqueous or organic environments. In this method, polymeric or hydrogel particles of desired shapes (e.g., small cubes) are initially loaded uniformly with an additive material (metal micro- or nanoparticles), which is then removed selectively by a chemical reaction propagating inwards from the particles’ surfaces (Fig. 1a). Coupling between reaction and diffusion makes the reaction front sharp and ultimately generates small structures inside of transparent particles – e.g., spheres inside of cubes or polyhedra inside of curvilinear particles (Fig. 2a and b). The emergence of these structures is described accurately by a three-dimensional RD model implemented using a finite element method (FEM, Fig. 1b) and applicable to arbitrary particle shapes. The CSPs fabricated via 3D RD can be further modified by chemical exchange of the cores (Fig. 2c–f), and can be assembled into larger structures, in which the cores are “suspended” in a transparent matrix (Fig. 3). These experiments suggest that the combination of “remote” fabrication based on 3D RD with self-assembly can provide a general route to micro-structured, open-lattice materials.

The $L = 400 \mu\text{m}$ to $L = 1 \text{ mm}$ particles (Fig. 1a) we used were made either from high-strength agarose (Omni Pur, EM Science, Darmstadt, Germany) or from poly(dimethylsiloxane) (PDMS, Sylgard 184, Dow Corning) by conventional molding^[10–13] against micropatterned masters and curing at room temperature. These materials were chosen because (i) in the absence of additives, they are optically transparent and (ii) they allow for a range of chemistries to be performed in their bulk in either aqueous (for agarose) or organic (for PDMS) solvents. The additives initially dispersed in the entire volume of the particles were electrolessly deposited copper colloids in agarose (colloid diameters ca. 15 nm by TEM; concentration of 31 mM in terms of Cu atoms) or gold nanoparticles (5.6 nm AuNPs; 38 mM in terms of Au atoms) in PDMS (for further details, see the Experimental section).

Immersion of the particles in a stirred solution of an appropriate etchant initiated a process, in which the metal colloids were oxidized to soluble metal salts that were subsequently cleared from the particles by diffusion. For agarose particles, the etchant was 100 mM aqueous solution of HCl under aerobic conditions (i.e., HCl/O₂), which reacted with copper to produce copper chloride, $2\text{HCl} + \text{Cu} + \frac{1}{2}\text{O}_2 \rightarrow \text{CuCl}_2 + \text{H}_2\text{O}$. For PDMS, a commercial, water-based Transene TFA gold etchant was mixed (1:1 v:v) with tetrahydrofuran (THF). The role of THF was to swell PDMS^[14] and allow the reactive I₃[−] to penetrate into the particle where it oxidized AuNPs into water-soluble [AuI₂][−] according to the $2\text{Au} + \text{I}^- + \text{I}_3^- \rightarrow 2[\text{AuI}_2]^-$ reaction.^[15] Both etching reactions were halted by removing the particles from their respective etchants and placing them into either an aqueous solution of NaBH₄/NaOH (for agarose/Cu particles) or a THF/water mixture (for PDMS/AuNP) to remove the unreacted etchant.

Upon immersion in the etchant solution, the etching reaction propagated inwards as a sharp front leaving behind a region of clear agarose/PDMS. Figure 1c and d illustrate such propagation into cubical agarose/Cu and PDMS/AuNP particles, respectively. In both cases, the sizes of the unetched regions (“the cores”) decrease with time of etching (front speed $\approx 18.5 \mu\text{m min}^{-1}$ in agarose/Cu and $\approx 1.6 \mu\text{m min}^{-1}$ in PDMS/AuNP; Fig. 1e), and their shapes gradually evolve from rounded cubes to spheres. These shape changes can be quantified in the form of a sphericity index, Φ (see caption to Fig. 1), calculated from the digitized projections of the cores and ranging from $\Phi = 1$ for a perfectly spherical core to $\Phi = 0$ for a cubical one. For both types of

[*] Prof. B. A. Grzybowski, P. J. Wesson, S. Soh, R. Klajn, K. J. M. Bishop
Department of Chemical and Biological Engineering
Northwestern University
2145 Sheridan Road, Evanston, IL 60208 (USA)
E-mail: grzybor@northwestern.edu
Prof. B. A. Grzybowski, T. P. Gray
Department of Chemistry
Northwestern University
2145 Sheridan Road, Evanston, IL 60208 (USA)

DOI: 10.1002/adma.200802964

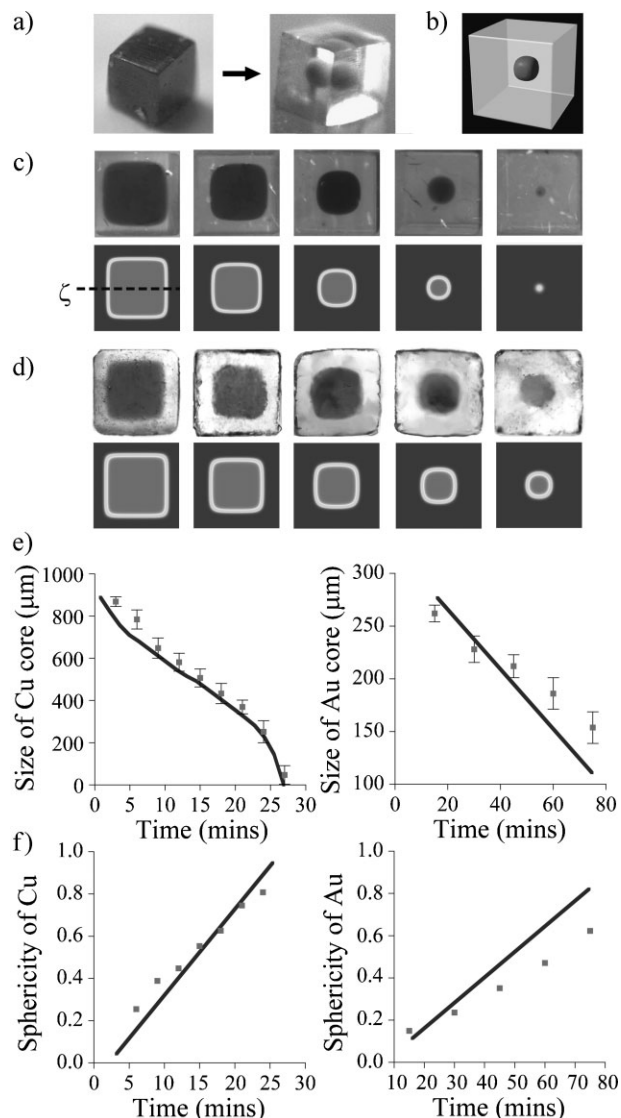


Figure 1. Fabrication by 3D RD. a) A small particle (here, a 1 mm agarose cube) is initially filled uniformly with Cu colloids. Upon immersion in an etchant solution, a sharp reaction-diffusion front propagates into the particle and ultimately “fabricates” a spherical core suspended in a clear agarose matrix. b) An example of a core-and-shell structure modeled by FEM method. Dark grey regions correspond to the high concentration of unetched metal in the core. c) The top row shows experimental, side-view images of 1 mm agarose/Cu cubes etched for 6, 12, 18, 24, and 27 min. Bottom row has the corresponding 2D projections of modeled 3D structures. d) Analogous experimental and simulated structures in 400 μm PDMS/AuNP cubes at 15, 30, 45, 60, and 75 min. e) Diameters of the Cu and AuNP cores as a function of time (measured along the dashed line ζ shown in (c)). f) Corresponding plots of the sphericity index Φ obtained from 2D core projections by (i) fitting a circle to an actual core shape, and (ii) calculating the difference, A , in area between the two; and (iii) calculating the value of $\Phi = (A_0 - A)/A_0$, where A_0 is the minimum area difference between the fitted circle and a square circumscribed about it. In this way, $\Phi = 1$ for a perfectly circular core and $\Phi = 0$ for a square one. In (e) and (f), the markers correspond to experimental data and the lines to the simulations. Standard deviations are based on the averages over at least ten cubes for each time point.

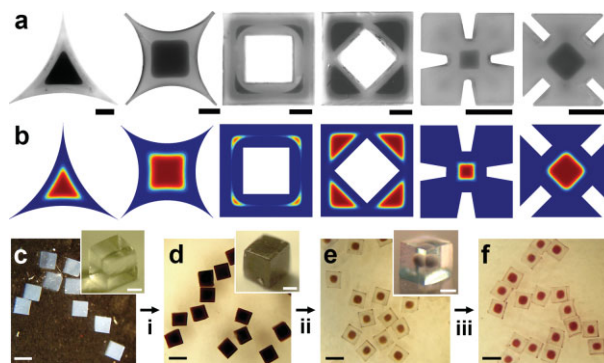


Figure 2. Examples of nonspherical cores generated by RD: a) triangular and square cores inside of particles with curved edges; multiple cores in “frame”-shaped particles; square cores in cross-shaped particles. Scale bars = 500 μm. b) The corresponding structures modeled with parameters described in the text for agarose/Cu system ($Da = 10^4$). c–f) Once fabricated, the cores can be exchanged “remotely” by galvanic replacement reactions. The specific sequence shows: c) 1 mm pure agarose cubes; d) cubes filled uniformly with copper colloids; e) Cu cores etched using HCl/O₂; and f) cores exchanged galvanically into gold-nanoparticle ones. Scale bars are 1 mm in the main images and 300 μm in the insets. The chemicals used are: (i) 1) SnCl₂, 2) H₂PdCl₄, 3) [Cu(tartrate)₂]²⁻, 4) NaBH₄; (ii) HCl, O₂; and (iii) HAuCl₄.

materials and for cubes of different sizes, the cores can be classified as spherical with $\Phi > 0.7$ when their diameters, d , are less than $\approx 40\%$ of the cube’s size, L . Also, the smallest cores we resolved were $\approx 10\%$ of the particles size (e.g., ≈ 40 μm in PDMS cubes). Statistics over sets of cubes etched for the same time reveal that the standard deviations, σ , of the core diameters at different times are 2.5–5% of the mean for agarose cubes and 2–6.7% for PDMS cubes, with the upper values corresponding to longest etching times. This polydispersity is minimal when the

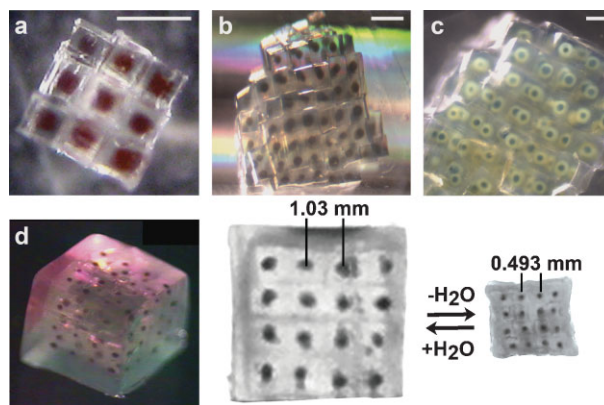


Figure 3. Three-dimensional assemblies of sphere-in-cube particles. a) A $3 \times 3 \times 3$ “supercube” made of 400 μm PDMS cubes with cores comprising 5.6 nm gold nanoparticles. b) An assembly of ca. 250 agarose cubes (500 μm) containing Cu cores, and c) 1 mm agarose cubes with Cu cores whose outer layers (greenish regions) were oxidized to CuCl. Scale bars = 1 mm. d) A $4 \times 4 \times 4$ supercube of 1 mm agarose cubes containing spherical Cu cores. This cube is encased in agarose. The supercube shrinks and expands when dried and re-hydrated. The change in linear dimensions is roughly by a factor of two.

cubes are vigorously agitated during etching. In the absence of or with gentle agitation, the polydispersity increases as the cubes stick to one another and/or to the walls of the container, causing them to be etched to different extents and less symmetrically than cubes fully exposed to the etching solution.

The key feature of the etching process is the sharpness of the RD front. Denoting the metal by the subscript M , and the etchant by E we have:

$$\partial C_E / \partial t = D \nabla^2 C_E - \alpha k C_E C_M$$

$$\partial C_M / \partial t = -\beta k C_E C_M \quad (1)$$

where C_M denotes the concentration of metal colloids/NP (in terms of atoms) immobilized in the cube, C_E stands for the concentration of etchant (limiting species), D is the diffusion coefficient of the etchant, k is the apparent reaction constant, and α and β are the stoichiometric coefficients for the etching reaction, $\alpha E + \beta M \rightarrow \text{Soluble Salt}$. These equations assume that metal particles do not diffuse through the agarose/PDMS matrix, and that the dissolved metal does not influence reaction kinetics or the transport of the fresh etchant. The initial and boundary conditions are such that: (i) the concentration of metal is initially uniform throughout the cube, C_M^0 , and (ii) the concentration of etchant is kept constant, C_E^0 , at the surface of the cube (since the solution is well-stirred). The RD equations can be further simplified by rescaling the variables: $\bar{C}_E = C_E / C_E^0$, $\bar{C}_M = C_M / C_M^0$, $\bar{x} = \mathbf{x} / L$, and $\bar{t} = Dt / L^2$, where L is a characteristic length of the gel/polymer particle (e.g., the side of a cube). This procedure yields the non-dimensional RD equations:

$$\partial \bar{C}_E / \partial \bar{t} = \nabla^2 \bar{C}_E - \alpha \text{Da} \bar{C}_E \bar{C}_M$$

$$\partial \bar{C}_M / \partial \bar{t} = -\beta \gamma \text{Da} \bar{C}_E \bar{C}_M \quad (2)$$

with initial conditions in the cube $\bar{C}_M(\mathbf{x}, 0) = 1$, $\bar{C}_E(\mathbf{x}, 0) = 0$, and boundary condition for the etchant concentration at the cube's surface, $\bar{C}_E(\mathbf{x}_S, t) = 1$ and $\gamma = C_E^0 / C_M^0$. The most important parameter in these equations is the dimensionless Damköhler number, $\text{Da} = kL^2 C_M^0 / D$, which here can be interpreted as a ratio of the characteristic width of the reaction zone, $L_{RZ} = (D/kC_M^0)^{1/2}$, to the dimensions of the cube, L , as $\text{Da} = (L/L_{RZ})^2$. Thus, the "sharpness" of the reaction zone, defined as L_{RZ}/L , may be expressed in terms of the Damköhler number as $\text{Da}^{-1/2}$. We note, however, that this relation between sharpness and Da holds only asymptotically as the front moves far from the initial boundaries of the cube; thus, for intermediate times, the other dimensionless parameter, γ , may also influence the sharpness.^[16]

For the case of agarose/Cu cubes, $\alpha = 1/2$, $\beta = 1$, and $C_M^0 = 31 \text{ mM}$. Since the etching process requires both HCl and O_2 (without oxygen, etching rates are much smaller^[17,18]), the effective etchant concentration is determined by the concentration of the limiting reagent, O_2 , dissolved in the etching solution

(from literature data, $\approx 8.4 \text{ mg L}^{-1}$ at 25°C ^[19]), $C_E^0 = 0.26 \text{ mM}$ such that $\gamma \approx 0.01$. The diffusion coefficient of oxygen through the gel matrix is also taken from literature,^[20] $D = 2.1 \times 10^{-9} \text{ m}^2 \text{ s}^{-1}$, as is the rate constant of the surface reaction, $k_S = 5.4 \times 10^{-4} \text{ m s}^{-1}$, determined previously^[18] for a planar Cu surface etched with 100 mM HCl/O_2 . For our system, however, this surface reaction rate has to be translated into a bulk etching rate accounting for the finite sizes of the colloidal particles (radii, $R \approx 5\text{--}10 \text{ nm}$). The procedure to do so is detailed in the Experimental section and gives a Damköhler number for the process, $\text{Da} \approx 10^4$.

For the PDMS/AuNP cubes, I_3^- is the reagent limiting gold etching. In this case, $C_M^0 = 38 \text{ mM}$ and $C_E^0 = 8 \text{ mM}$ such that $\gamma \approx 0.2$; other parameters are $\alpha = 1/2$, $\beta = 1$, and $D = 5 \times 10^{-12} \text{ m}^2 \text{ s}^{-1}$.^[21] Using the experimentally estimated rate constant for AuNP etching, $k_S = 1.4 \times 10^{-6} \text{ m s}^{-1}$, the Damköhler number for $L = 400 \mu\text{m}$ cubes is then estimated at $\text{Da} \approx 6200$.

The fits in Figure 1e and f show that when the non-dimensional RD Equations 2 are solved numerically (using the Fluent Finite Element Method) with the estimated Damköhler numbers; they give good quantitative agreement both in terms of the time evolution of the cores as well as their sphericities. Interestingly, the combination of core "sharpness" (i.e., narrow reaction zone) and high sphericity is observed only for intermediate values of $\text{Da} \approx 10^4$. When Da is smaller, e.g., of order 10^3 , the width of the reaction zone is roughly $\text{Da}^{-1/2}$ or 3% of the cube size, such that the contours of the cores – albeit more spherical – are significantly "blurred." In contrast, for high values of $\text{Da} \approx 10^6$, etching becomes increasingly diffusion limited, and the etchant delivered to the reaction front is consumed immediately (see Supporting Information Fig. S1). As a result, the reaction front is sharp ($\approx 0.1\%$ of L), but resembles more the initial, cubical contour.

For particles other than cubical, the RD process can generate cores of different shapes or even several cores per particle. This is shown in Figure 2, which has the experimental images (Fig. 2a) and the corresponding calculated contours (Fig. 2b) of CSPs of various shapes. The two leftmost examples illustrate a transformation of a curvilinear particle contour into a polygonal core and demonstrate that RD – with proper design of the curvature of the particle's boundary – is not limited to etching rounded shapes. The third and fourth examples show that in particles with sharp internal corners, the RD fronts can "break up" and produce multiple, separate cores in one particle. Finally, the two rightmost examples show particles having inward-pointing "cuts" that control the angular orientation of the square cores. The fact that the our simple RD model reproduces the experimentally developed cores indicates that in a well stirred solution, any diffusion limitations on the delivery of fresh etchant into these cuts can be neglected.

Once fabricated, the cores can be further modified "remotely" by galvanic replacement reactions (Fig. 2c). For example, when an agarose cube containing a copper core is immersed in 20 mM aqueous solution of $\text{HAuCl}_4 \cdot 3\text{H}_2\text{O}$, the following red-ox reaction takes place: $2\text{AuCl}_4^- + 3\text{Cu} \rightarrow 2\text{Au} + 3\text{Cu}^{2+} + 8\text{Cl}^-$. Since the difference in standard potentials, $E^0 = \varepsilon_{\text{AuCl}_4^-/\text{Au}}^0 - \varepsilon_{\text{Cu}^{2+}/\text{Cu}}^0 = 0.663 \text{ V}$, is positive, this reaction transforms the copper colloids in the cores into gold ones. Importantly, metal exchange that occurs does not affect either the size or the shape of the core, and

manifests itself by a color change of the core from brown (copper, Fig. 2e) to red (gold; Fig. 2f). Because the equilibrium constant for the reaction is very high ($K_{eq} = e^{\frac{nFE^0}{RT}} = 10^{67}$, where $n=6$ is the number of electrons exchanged in the reaction, and F is the Faraday constant), the exchange reaction is quantitative as verified by elemental analysis of the colloids comprising the cores. Since the procedure can be extended to other metals having standard redox potentials higher than that of copper (i.e., $\epsilon_{Me^{n+}/Me}^0 > \epsilon_{Cu^{2+}/Cu}^0$), we were also able to fabricate particles comprising silver ($\epsilon_{Ag^+/Ag}^0 = +0.800$ V), palladium ($\epsilon_{Pd^{2+}/Pd}^0 = +0.915$ V) and platinum ($\epsilon_{Pt^{2+}/Pt}^0 = +1.188$ V) cores. Other metals that could be used for the galvanic replacement include rhodium, iridium, tellurium and others. An interesting variation of the method is that under some conditions, the chemical modification of the cores can be only partial and can produce double-layer cores, as illustrated in Figure 3c, where only the outer portions of the copper cores were oxidized to copper(I) chloride.

The core-and-shell particles can be used as building blocks for higher-order structures, in which the opaque cores are separated and “suspended” in a transparent matrix. As a proof-of-concept experiment, we assembled (after etching) spheres-in-cubes into aggregates containing tens to hundreds of CSP. Figure 3 shows such assemblies made of 400 μ m PDMS/AuNP cubes (Fig. 3a), 1 mm Agarose/Cu cubes (Fig. 3b), and 1 mm agarose cubes having two-shell Cu/CuCl cores (Fig. 3c; prepared by partial oxidation of Cu cores). The PDMS structures were assembled by gentle agitation on an orbital shaker (Bellco Glass SH-542) in a mixture of acetonitrile and 1-octadecene whose 1250:1 v/v ratio provided optimal hydrophobic “contrast” between hydrophobic PDMS and polar solvent (with pure acetonitrile, the cubes rapidly clumped into disorder structures; with too much 1-octadecene, the particles did not form large assemblies). For the Agarose/Cu system, the optimal procedure for self-assembly involved transferring the cubes into acetone and then adding 5% v/v hexane while gently shaking the solution. The assembled structures were made permanent by immersing them in either liquid PDMS prepolymer or in hot agarose that were subsequently cured/allowed to gel at room temperature. One interesting property of such stable assemblies is shown in Figure 3d, where a $4 \times 4 \times 4$ “supercube” can be reversibly shrunken and expanded upon drying and rehydrating the agarose matrix.

In summary, we described an experimental method that uses reaction-diffusion to fabricate structures comprising colloidal-metals inside of permeable particles. With the help of the RD model we developed, this procedure can be used to fabricate a variety of complex shapes and structures, and can be combined with self-assembly to arrange the core-and-shell particles into open-lattice crystals. If the constituent particles were further miniaturized, such crystals could be useful as diffractive elements. Application of the 3D RD method to smaller particles, however, requires better control of reaction-diffusion at small scales and, likely, slower reaction rates and smaller diffusion coefficients. Future research could also extend the RD approach to particles supporting several chemistries/metals at the same time, where different metal etchants would perform independent fabrication tasks to yield topologically complex cores.

Experimental

Agarose/Cu Particle Preparation: Agarose/Cu particles were prepared by casting a hot 8% solution of high gel strength OmniPur agarose against an oxidized PDMS master [11–13] and pressing the PDMS against an 85 °C glass slide to remove excess agarose solution. After gelation at room temperature, the cubes were removed from the mold by soaking the PDMS in hexanes and bending the mold. Once liberated, the pieces were soaked in a sensitizing solution (26 mM SnCl₂ and 0.47 M HCl in water) for 2 h, transferred directly to an activating solution (2.8 mM PdCl₂ and 0.12 M HCl in water) for 30 min, followed by soaking in a 31 mM CuSO₄ water solution containing 0.22 M KOH and 89 mM potassium sodium tartrate for 2 h. To reduce copper salt to colloidal Cu⁰ particles, the cubes were transferred into an aqueous sodium borohydride solution (0.21 M) in 0.18 M KOH and shaken for 6–8 h. This procedure gave brownish cubes uniformly doped with colloidal copper particles. Average size of these particles (≈ 15 nm) was determined by TEM of thin slices of the loaded agarose particles.

PDMS/Au Particle Preparation: PDMS/AuNP particles were made as follows. First, ≈ 5.6 nm gold nanoparticles stabilized by dodecylamine [22] were functionalized with alkyl thiols by soaking in a 1:1 mol:mol ethanol solution of octanethiol and hexadecanethiol (1.3 mM total thiol concentration). A mixture of short- and long-chain thiols in the formed SAMs rendered the NPs soluble in the PDMS prepolymer while allowing for NP etching (NPs covered with monocomponent SAMs of short octanethiol aggregated; those stabilized with SAMs of long hexadecanethiol were resistant to etching). Nanoparticles were precipitated with methanol and washed five times with methanol to remove excess thiols and surfactants. The resulting black solid was re-suspended in petroleum ether to give a deep-red solution that was mixed into Sylgard-184 poly(dimethylsiloxane) (PDMS) pre-polymer. Petroleum ether was evaporated by stirring and heating at 65 °C for 1.5 h. Sylgard-184 curing agent was added to the AuNP/prepolymer mixture, which was then cast against cubical wells of a micropatterned agarose master (prepared as described previously in ref. [11–13]). PDMS was degassed under vacuum, its excess was removed from the master’s surface using a razor blade, and the remaining portion was cured at room temperature overnight (in a sealed container to prevent drying of the agarose). Soaking in methylene chloride caused swelling of the cured PDMS cubes and facilitated their removal from the master’s wells. The cubes were reddish-purple and had the AuNPs uniformly dispersed throughout their volumes. Importantly, for concentrations of AuNP less than 1.7 mM (in terms of gold atoms per unit volume of PDMS), the particles were not aggregated as evidenced by the location of Au SPR band, $\lambda_{max} \approx 520$ nm, in the cured PDMS.

Transformation of the Surface Etching Rates into Apparent Bulk Rates: Values for reaction rates describing metal etching are usually expressed in terms of the velocity of the receding surface of a bulk metal, $d\delta/dt$, with units of length per time. If the etching rate is first order with respect to the etchant of concentration, C_E , the velocity of the receding surface can be written as: $\nu^{-1}(d\delta/dt) = k_S C_E$, where ν is the molar volume of the bulk metal, and k_S is the surface rate constant of the etching reaction. Also, if the experimental values of this velocity are reported as $(d\delta/dt)_0$ for a given etchant concentration, C_E^0 , the rate constant may be estimated as $k_S = (d\delta/dt)_0 / \nu C_E^0$.

These experimentally measured *surface* rate constants can be translated into the apparent *bulk* rate constants describing the dissolution of finite-sized colloidal particles immersed in the gel matrix. To do so, we first consider the etching of a single spherical particle of radius, R , and containing N metal atoms, related to R as $N = \frac{4}{3}\pi R^3/\nu$. The etching rate may be defined as $(4\pi R^2)^{-1}(dN/dt) = \nu^{-1}(dR/dt) = -k_S C_E$. Integrating this expression, we find that for $0 \leq t \leq R_0/k_S \nu C_E$, the radius of the particle evolves as $R = R_0 - k_S \nu C_E t$, where R_0 is the initial radius of the nanoparticle. Substituting this expression back into the rate equation, we can write $dN/dt = -4\pi k_S C_E (R_0 - k_S \nu C_E t)^2$. Because this rate varies with t , we integrate it over the period $R_0/k_S \nu C_E$ required to etch the entire particle. This procedure yields the *average* rate of particle etching: $\langle dN/dt \rangle = -4\pi R_0^3 k_S C_E / 3$. Now, for a collection of colloidal particles dispersed in some matrix, the rate at which metal atoms are consumed by the etching reaction is simply equal to the average rate for a single colloid times the total number of particles, N_p ,

in solution, $dN_M/dt = \langle dN/dt \rangle N_P$. Here, the number of colloidal particles, N_P , is related to the number of metal atoms, N_M , as $N_M = (4\pi R_0^3/3v)N_P$, where $4\pi R_0^3/3v$ is simply the number of atoms in a single particle of radius R_0 . Substituting this relation into the above equation and dividing by the total volume, V , we obtain, $dC_M/dt = -(k_S v/R_0)C_M C_E$. This rate equation, which describes how the total concentration of metal atoms, C_M , evolves in time, is identical to the second order rate equations introduced in Equation 1 in the text. Thus, by inspection, we can identify $k = k_S v/R_0$ as the apparent bulk rate constant for the dissolution of metal atoms into soluble ions. Also, the Damköhler number for the RD process of core formation, defined in the main text as $Da = kL^2 C_M^0/D$, may now be related to the surface reaction rate as

$$Da = \frac{k_S v L^2 C_M^0}{DR_0}$$

Acknowledgements

B. G. gratefully acknowledges support from the NSF Career grant(CTS-0547533). R. K. was supported in part by the MRSEC program of the National Science Foundation (DMR-0520513) at the Materials Research Center of Northwestern University. K. B. was supported in part by a NSF Graduate Research Fellowship. Supporting Information is available online from Wiley InterScience or from the author.

Received: October 8, 2008
Published online: March 6, 2009

-
- [1] J. de Jong, R. G. H. Lammertink, M. Wessling, *Lab Chip* **2006**, *6*, 1125.
[2] J. C. McDonald, D. C. Duffy, J. R. Anderson, D. T. Chiu, H. K. Wu, O. J. A. Schueller, G. M. Whitesides, *Electrophoresis* **2000**, *21*, 27.
[3] D. B. Weibel, W. R. DiLuzio, G. M. Whitesides, *Nat. Rev. Microbiol.* **2007**, *5*, 209.

- [4] L. Y. Chu, A. S. Utada, R. K. Shah, J. W. Kim, D. A. Weitz, *Angew. Chem. Int. Ed.* **2007**, *46*, 8970.
[5] A. S. Utada, E. Lorenceau, D. R. Link, P. D. Kaplan, H. A. Stone, D. A. Weitz, *Science* **2005**, *308*, 537.
[6] J. W. Kim, A. S. Utada, A. Fernandez-Nieves, Z. B. Hu, D. A. Weitz, *Angew. Chem. Int. Ed.* **2007**, *46*, 1819.
[7] C. J. Gerdtts, V. Tereshko, M. K. Yadav, I. Dementieva, F. Collart, A. Joachimiak, R. C. Stevens, P. Kuhn, A. Kossiakoff, R. F. Ismagilov, *Angew. Chem. Int. Ed.* **2006**, *45*, 8156.
[8] M. Seo, C. Paquet, Z. H. Nie, S. Q. Xu, E. Kumacheva, *Soft Matter* **2007**, *3*, 986.
[9] M. Fialkowski, A. Bitner, B. A. Grzybowski, *Nat. Mater.* **2005**, *4*, 93.
[10] Y. N. Xia, J. J. McClelland, R. Gupta, D. Qin, X. M. Zhao, L. L. Sohn, R. J. Celotta, G. M. Whitesides, *Adv. Mater.* **1997**, *9*, 147.
[11] K. J. M. Bishop, T. P. Gray, M. Fialkowski, B. A. Grzybowski, *Chaos* **2006**, *16*, 037102.
[12] C. J. Campbell, R. Klajn, M. Fialkowski, B. A. Grzybowski, *Langmuir* **2005**, *21*, 418.
[13] C. J. Campbell, S. K. Smoukov, K. J. M. Bishop, B. A. Grzybowski, *Langmuir* **2005**, *21*, 2637.
[14] J. N. Lee, C. Park, G. M. Whitesides, *Anal. Chem.* **2003**, *75*, 6544.
[15] Y. Nakao, K. Sone, *Chem. Commun.* **1996**, 897.
[16] Z. Koza, *Phys. A* **1997**, *240*, 622.
[17] L. Burzynska, A. Maraszewska, Z. Zembura, *Corros. Sci.* **1996**, *38*, 337.
[18] A. M. S. El Din, M. E. El Dahshan, A. M. T. El Din, *Desalination* **2000**, *130*, 89.
[19] *Standard Methods for the Examination of Water and Wastewater*, 12th ed. (Ed: H. P. Orland), American Public Health Association, New York, USA **1965**.
[20] A. C. Hulst, H. J. H. Hens, R. M. Buitelaar, J. Tramper, *Biotechnol. Tech.* **1989**, *3*, 199.
[21] M. M. Santore, M. J. Kaufman, *J. Polym. Sci. Part B* **1996**, *34*, 1555.
[22] A. M. Kalsin, M. Fialkowski, M. Paszewski, S. K. Smoukov, K. J. M. Bishop, B. A. Grzybowski, *Science* **2006**, *312*, 420.